ELSEVIER

Journal of Organometallic Chemistry 658 (2002) 50–61

Journal of Organometallic Chemistry

www.elsevier.com/locate/jorganchem

Rhenium tricarbonyl complexes of tris(pyrazolyl)methane ligands: first structural characterization of an isomer pair of tris(pyrazolyl)methane derivatives and the supramolecular structure of the homobimetallic complex {1,4-$C_6H_4[CH_2OCH_2C(pz)_3]_2[Re(CO)_3]_2\}(Br)_2$

Daniel L. Reger *, Kenneth J. Brown, Mark D. Smith

Department of Chemistry and Biochemistry, University of South Carolina, Columbia, SC 29208, USA

Received 15 April 2002; received in revised form 17 May 2002; accepted 17 May 2002

Abstract

The reaction of either $HC(pz)_3$, $HC(3,5\text{-}Me_2pz)_3$, $HC(3\text{-}Phpz)_3$, or a 4:1 $HC(3\text{-}i\text{-}Prpz)_3$–$HC(3\text{-}i\text{-}Prpz)_2(5\text{-}i\text{-}Prpz)$ mixture (pz = pyrazolyl ring) and $Re(CO)_5Br$ results in the formation of $\{[HC(pz)_3]Re(CO)_3\}Br$ (**1**), $\{[HC(3,5\text{-}Me_2pz)_3]Re(CO)_3\}Br$ (**3**), $\{[HC(3\text{-}Phpz)_3]Re(CO)_3\}Br$ (**4**), $\{[HC(3\text{-}i\text{-}Prpz)_3]Re(CO)_3\}Br$ (**5**), and $\{[HC(3\text{-}i\text{-}Prpz)_2(5\text{-}i\text{-}Prpz)]Re(CO)_3\}Br$ (**6**). The reaction of $PhC(pz)_2(py)$ (py = pyridyl ring) and $Re(CO)_5Br$ yields $\{[PhC(pz)_2(py)]Re(CO)_3\}Br$ (**9**) while a reaction of $Re(CO)_5Br$ and 1,4-$C_6H_4[CH_2OCH_2C(pz)_3]_2$ in a 2:1 mol ratio gives $\{1,4\text{-}C_6H_4[CH_2OCH_2C(pz)_3]_2[Re(CO)_3]_2\}(Br)_2$ (**10**). The reaction of $Re(CO)_5Br$ and $AgBF_4$ followed by addition of either $HC(pz)_3$ or the 4:1 $HC(3\text{-}i\text{-}Prpz)_3$–$HC(3\text{-}i\text{-}Prpz)_2(5\text{-}i\text{-}Prpz)$ mixture results in the preparation of $\{[HC(pz)_3]Re(CO)_3\}BF_4$ (**2**), $\{[HC(3\text{-}i\text{-}Prpz)_3]Re(CO)_3\}BF_4$ (**7**), and $\{[HC(3\text{-}i\text{-}Prpz)_2(5\text{-}i\text{-}Prpz)]Re(CO)_3\}BF_4$ (**8**), respectively. The carbonyl stretching frequencies in all of these complexes are similar, with the exception of **9**, which has much lower values. The methine hydrogen atoms of compounds **1**, **5**, and **6** show deshielded chemical shift values as a result of hydrogen-bonding interactions with the bromide counterion. The solid state structures of the isomeric pair **5** and **6** have very similar bond angles and distances about the metal and show weak hydrogen-bonding interactions between the Br^- anion and the methine hydrogen. The structure of the bimetallic complex, **10**, in which two $[Re(CO)_3]^+$ units are linked by the bitopic ligand, is organized by π–π and (C)H···π interactions into a two-dimensional supramolecular network of two interpenetrating 'zigzag' chains. © 2002 Published by Elsevier Science B.V.

Keywords: Tris(pyrazolyl)methane ligands; Rhenium carbonyl complexes; Supramolecular structure

1. Introduction

We have been exploring the chemistry of metal complexes of tris(pyrazolyl)methane ligands [1], a tripodal neutral ligand set isoelectronic with the more heavily studied tris(pyrazolyl)borate ligands [2]. The primary reason the tris(pyrazolyl)methane ligands have not been studied as extensively as the tris(pyrazolyl)borate ligands is that their preparations have been more difficult, and 'second generation' tris(pyrazolyl)methane ligands with bulky substituents at the third-position of the pyrazolyl ring have only recently been synthesized [3]. We have recently reported substantial improvements in the preparations of these ligands and have developed chemistry where the central methine carbon atom can be functionalized with groups other than a hydrogen atom [3c].

* Corresponding author. Tel.: +1-803-777-2587; fax: +1-803-777-9521

E-mail address: reger@mail.chem.sc.edu (D.L. Reger).

0022-328X/02/$ - see front matter © 2002 Published by Elsevier Science B.V.
PII: S0022-328X(02)01620-0

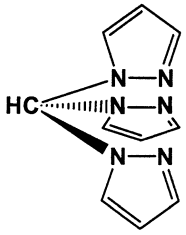

tris(1-pyrazolyl)methane

We are interested in using these ligands to develop new organometallic compounds of rhenium due to potentially interesting electrochemical, photophysical, and photochemical properties that make them promising candidates for 'next-generation' optical switches and chemical sensors [4]. In addition, the favorable nuclear properties of the β-emitting nuclides ^{188}Re ($t_{1/2} = 16.94$ h) and ^{186}Re ($t_{1/2} = 3.78$ days) have spawned interest in their potential use as therapeutic agents in nuclear medicine [4c–e]. Previously, we have reported the syntheses of a series of manganese tricarbonyl complexes containing the tris(pyrazolyl)methane ligands [3c]. The complexes were synthesized in high yield and were found to be very stable. The only analogous report in rhenium chemistry is the very recent communication of the solid state structures of {[HC(pz)$_3$]Re(CO)$_3$}Br and {[MeC(pz)$_3$]Re(CO)$_3$}I [5].

Reported here are the syntheses of the series of complexes $[LRe(CO)_3]^+$ (L = HC(pz)$_3$, HC(3,5-Me$_2$-pz)$_3$, HC(3-Phpz)$_3$, HC(3-*i*-Prpz)$_3$, HC(3-*i*-Prpz)$_2$-(5-*i*-Prpz), PhC(pz)$_2$(py)) (pz = pyrazolyl ring, py = pyridyl ring). We report the structural characterizations of the first complexes that contain an isomeric pair of tris(pyrazolyl)methane ligands, {[HC(3-*i*-Prpz)$_3$]Re-(CO)$_3$}Br and {[HC(3-*i*-Prpz)$_2$(5-*i*-Prpz)]Re(CO)$_3$}Br. An additional driving force for this research is our recent development of ether-linked bitopic tris(pyrazolyl)methane ligands, such as 1,4-C$_6$H$_4$[CH$_2$-OCH$_2$C(pz)$_3$]$_2$ [6], that allow for the syntheses of bimetallic species and coordination polymers that should have very interesting physical properties. To this end, we report here the synthesis and supramolecular structure of {1,4-C$_6$H$_4$[CH$_2$OCH$_2$C(pz)$_3$]$_2$-[Re(CO)$_3$]$_2$}(Br)$_2$.

2. Results and discussion

The reaction between Re(CO)$_5$Br and either HC(pz)$_3$, HC(3,5-Me$_2$pz)$_3$, HC(3-Phpz)$_3$, or a 4:1 HC(3-*i*-Prpz)$_3$–HC(3-*i*-Prpz)$_2$(5-*i*-Prpz) mixture in toluene results in the formation of {[HC(pz)$_3$]Re(CO)$_3$}Br (**1**), {[HC(3,5-Me$_2$pz)$_3$]Re(CO)$_3$}Br (**3**), {[HC(3-Phpz)$_3$]Re(CO)$_3$}Br (**4**), {[HC(3-*i*-Prpz)$_3$]Re(CO)$_3$}Br (**5**), and {[HC(3-*i*-Prpz)$_2$(5-*i*-Prpz)]Re(CO)$_3$}Br (**6**) (Eq. (1)).

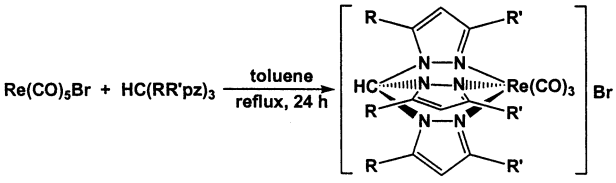

(1)

A similar reaction between PhC(pz)$_2$(py) and Re(CO)$_5$Br yields {[PhC(pz)$_2$(py)]Re(CO)$_3$}Br (**9**), while the reaction between Re(CO)$_5$Br and 1,4-C$_6$H$_4$[CH$_2$OCH$_2$C(pz)$_3$]$_2$ in a 2:1 mol ratio gives the corresponding homobimetallic derivative, {1,4-C$_6$H$_4$[CH$_2$OCH$_2$C(pz)$_3$]$_2$ [Re(CO)$_3$]$_2$}Br$_2$ (**10**) (Eq. (2)).

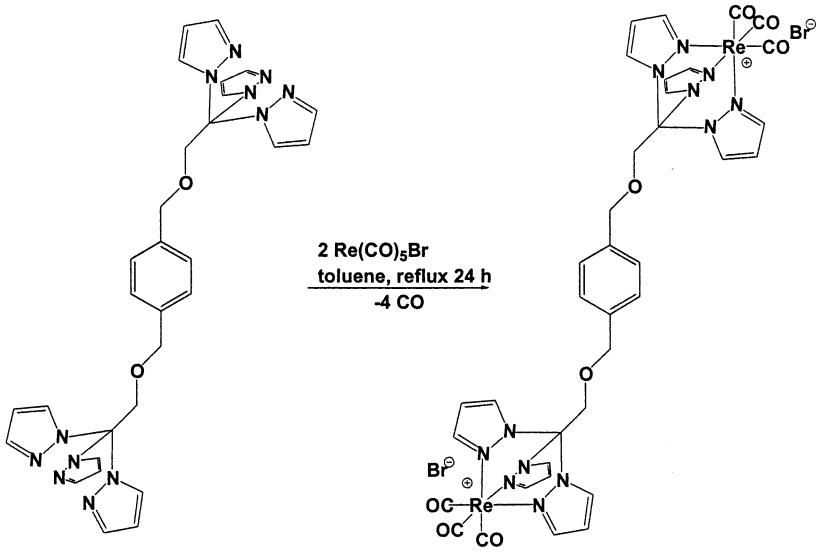

(2)

The reaction between $Re(CO)_5Br$ and $AgBF_4$ followed by reaction with either $HC(pz)_3$ or the 4:1 HC(3-*i*-Prpz)$_3$–HC(3-*i*-Prpz)$_2$(5-*i*-Prpz) mixture results in the formation of {[$HC(pz)_3$]$Re(CO)_3$}BF_4 (**2**), {[HC(3-*i*-Prpz)$_3$]$Re(CO)_3$}BF_4 (**7**), and {[HC(3-*i*-Prpz)$_2$(5-*i*-Prpz)]$Re(CO)_3$}BF_4 (**8**), respectively. All of the complexes are air and thermally stable up to 200 °C and are soluble in acetone, acetonitrile, and methylene chloride, but insoluble in aliphatic solvents.

The reaction between the HC(3-*i*-Prpz)$_3$–HC(3-*i*-Prpz)$_2$(5-*i*-Prpz) mixture, a mixture that has not been separated, and $Re(CO)_5Br$ was carried out with a slight excess of the ligands, while the reaction to form the BF_4^- derivative was done in a 1:1 mol ratio. In either case, the symmetrical, **5** and **7**, and asymmetrical complexes, **6** and **8**, formed during the reactions. These results contrast our previous report in the analogous manganese system [3c] where only the symmetrical ligand complex was formed in reactions that used an excess of the mixture of ligands. In the $Re(CO)_5Br$ reaction, the product was a 5.7–1 mixture of **5**–**6**, a mixture that could not be separated by recrystallization. Crystals suitable for X-ray analysis formed when the mixture was dissolved in acetone and allowed to slowly evaporate. Individual crystals of **5** and **6** were physically separated from this mixture for the X-ray studies. In the case of the BF_4^- complexes, recrystallization of the crude 4/1 mixture of **7**–**8** from a methylene chloride–hexane mixture yields pure **7** in low yield.

The IR stretching frequencies for the carbonyl ligands for complexes **1**–**10** are provided in Table 1. The carbonyl stretching vibrations of complexes **1**–**8** and **10** are comparable and occur within a few wave numbers of one another. The complexes with alkyl-substituted ligands have slightly lower values as would be expected because of the electron donating substituents, but the differences are only a few wavenumbers. The only exception is the {[$PhC(pz)_2(py)$]$Re(CO)_3$}(Br) complex, **9**, which has much lower values. This result can be attributed to the more basic nature of the pyridyl ring, which also breaks the local C_{3v} symmetry of the $Re(CO)_3$ unit resulting in a splitting of the E mode. In our previous work [3c], the {[tris(pyrazolyl)methane]$Mn(CO)_3$}(CF_3SO_3) complexes and {[$PhC(pz)_2$(py)]$Mn(CO)_3$}(CF_3SO_3) all showed only small variations in the carbonyl stretching vibrations. The surprising result is not that the more basic pyridyl ring influences the carbonyl stretching frequencies of {[$PhC(pz)_2(py)$]$Re(CO)_3$}(Br), but that it does not influence those of {[$PhC(pz)_2(py)$]$Mn(CO)_3$}(CF_3SO_3) to a greater extent.

A very interesting result was found in the ^{1}H-NMR shifts of the methine hydrogen atoms of the complexes, Table 1. The methine hydrogen of compounds **1**, **5**, and **6**, which all have bromide as the counterion, show very unusual chemical shifts of 13.04, 12.69, and 12.09 ppm, respectively. These shifts are deshielded from that observed with the uncomplexed ligand by 4.31, 4.30, and 3.69 ppm, respectively. The analogous compounds **2**, **7**, and **8** containing the same cations, respectively, but BF_4^- as the counter ion, show much less dramatic chemical shifts of 9.88, 9.47, and 9.53 ppm, which are only deshielded from the uncomplexed ligand by 1.15, 1.08, and 1.13 ppm, respectively. A similar trend was also seen by Seymore and Brown [7] in the study of {[$HC(pz)_3$]$ReOCl_2$}X complexes (X = Cl and BF_4). Their Cl^- complex has a methine proton shift of 12.54 ppm, while the BF_4^- complex has a shift of 9.19 ppm. Our data suggests that the Br^- counterion interacts in solution with the methine hydrogen atom forming a weak hydrogen-bonding interaction. The BF_4^- counter ion does not interact as strongly, and, therefore, does not deshield the methine hydrogen atom as strongly.

The ^{13}C-NMR chemical shifts are also influenced by this interaction. In this case, the methine carbon for the

Table 1
IR, ^{1}H-, and ^{13}C-NMR data for complexes **1**–**10**

Complex	IR ν(CO) cm^{-1}	^{1}H (*HC*) ppm (Δ [a])	^{13}C (H*C*) ppm (Δ [b])
{[$HC(pz)_3$]$Re(CO)_3$}Br (**1**)	2042, 1938	13.04(4.31)	73.9(9.2)
{[$HC(pz)_3$]$Re(CO)_3$}BF_4 (**2**)	2043, 1938	9.88(1.15)	77.1(6.0)
{[$HC(3,5\text{-}Me_2pz)_3$]$Re(CO)_3$}Br (**3**)	2036, 1930	8.31(0.11)	
{[$HC(3\text{-}Phpz)_3$]$Re(CO)_3$}Br (**4**)	2040, 1934	10.68(1.82)	
{[HC(3-*i*-Prpz)$_3$]$Re(CO)_3$}Br (**5**)	2037, 1930	12.69(4.30)	73.6(9.5)
{[HC(3-*i*-Prpz)$_2$(5-*i*-Prpz)]$Re(CO)_3$}Br (**6**)	2037, 1930	12.09(3.69)	
{[HC(3-*i*-Prpz)$_3$]$Re(CO)_3$}BF_4 (**7**)	2037, 1932	9.47(1.08)	77.2(5.9)
{[HC(3-*i*-Prpz)$_2$(5-*i*-Prpz)]$Re(CO)_3$}BF_4 (**8**)	2037, 1932	9.53(1.13)	
{[$PhC(pz)_2(py)$]$Re(CO)_3$}Br (**9**)	2026, 1922, 1899	N/A	N/A
{1,4-C_6H_4[$CH_2OCH_2C(pz)_3$]$_2$[$Re(CO)_3$]$_2$}$(Br)_2$ (**10**)	2042, 1938	N/A	N/A

[a] The number in parenthesis is the difference in the ^{1}H shift between the metal complex and the corresponding proton in the free, uncoordinated ligand [3c].

[b] The number in parenthesis is the difference in the ^{13}C shift between the metal complex and the corresponding carbon in the free, uncoordinated ligand [3c].

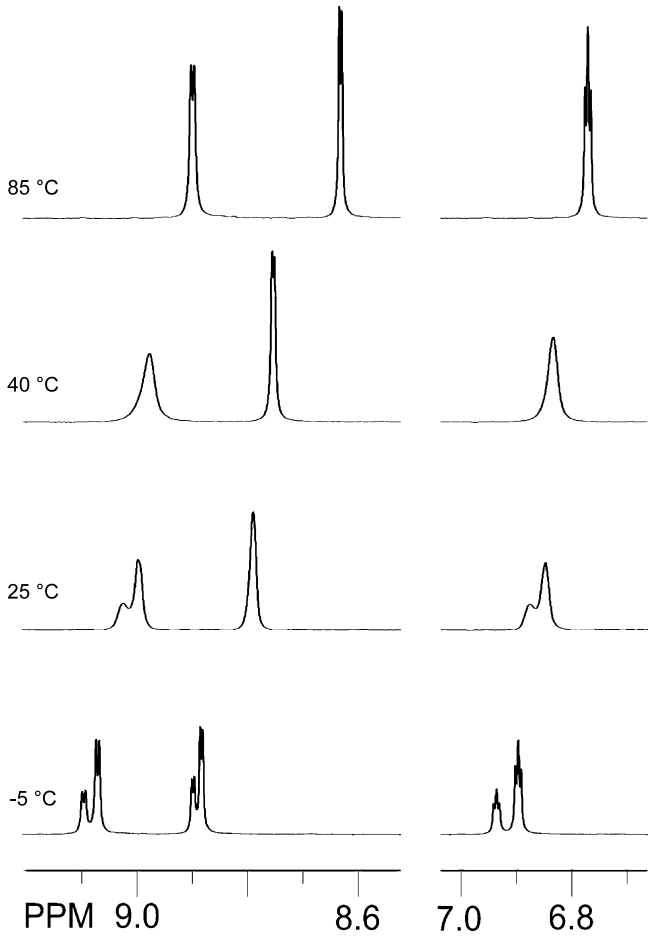

Fig. 1. Variable temperature ^{1}H-NMR spectra of the pyrazolyl hydrogen atoms for {1,4-C_6H_4[$CH_2OCH_2C(pz)_3$]$_2$[$Re(CO)_3$]$_2$}$(Br)_2$.

three bromide complexes are substantially more shielded, when compared with that in the free ligand and that observed in the BF_4^- complexes. The results of the NMR experiments are supported by the solid-state structures, vide infra. Also, the most shielded, least shifted from free ligand, methine hydrogen resonance is in {[HC(3,5-Me_2pz)$_3$]Re(CO)$_3$}Br (**3**), where the 5-methyl substituents sterically prevent any type of hydrogen-bonding interaction with the methine hydrogen atom.

A variable temperature ^{1}H-NMR spectroscopic study of **10** (Fig. 1) in DMF revealed that at low temperatures each type of hydrogen atom on the pyrazolyl rings appears as two resonances in a 2/1 ratio. This result is consistent with the solid state structure of **10** (vide infra, see Fig. 4) where the oxygen atom of the ether linkage straddles two of the pyrazolyl rings and is anti with respect to the third. Upon warming, the resonances broaden and coalesce, such that at 85 °C only one resonance for each type of pyrazolyl hydrogen is observed. The high temperature spectrum showing equivalent pyrazolyl rings on the NMR time scale is similar to the room temperature spectrum of the free ligand, although the solid state structure of the free ligand also shows non-equivalent pyrazolyl rings [6]. Given the inert nature of rhenium–carbon and rhenium–nitrogen bonds in **10**, the fluxional process responsible for the equilibration of the pyrazolyl rings is rotation about the central carbon atom of the tris(pyrazolyl)methane unit (C1 in Fig. 4) and the CH_2(C2) bonded to it. Coordination of the rings to the rhenium aligns the hydrogen atoms in the 5-position of the pyrazolyl rings toward the $-CH_2OCH_2R$ linker, causing a barrier to rotation about the central C(C1)–CH_2(C2) bond**.** In the free ligand, the pz rings are rotated to minimize this interaction [6]. The energy barrier, $\Delta G^{\ddagger}$, of 15.5 ± 0.5 kcal mol^{-1}, associated with this process for **10** was calculated by using the expression described by Kessler but with the rate constant modified for an unsymmetrical two-site exchange [8].

2.1. Solid State Structures

Figs. 2 and 3 show ORTEP diagrams of **5** and **6** and selected bond distances and angles are collected in Table 2. Fig. 2 shows cation **A**, one of the three nonequivalent forms present in the crystal of **5**. For each cation, three nitrogen atoms from the ligand and three carbon atoms from the carbonyl ligands surround the rhenium in a nearly octahedral arrangement. The average Re–N distance is 2.19 Å for **5** and 2.18 Å for **6**. Despite nearly identical averages, the 5-*i*-Prpz ring in **6** has a Re–N bond distance of 2.15 Å, ca. 0.04 Å shorter than the average for **5**. Presumably, this bond is slightly shorter due to the reduction of steric interactions caused by the absence of the bulky isopropyl group located at the third-position of the pyrazolyl ring. This steric difference is not reflected in the bond angles where the average N–Re–N angles are 82° for both **5** and **6**, and the average C–Re–C angle for the carbonyl groups are 88° for **5** and 89° for **6**. These angles and distances are consistent with the recent report of the structures of **1** and [$MeC(pz)_3$]Re(CO)$_3$}I [5].

Weak hydrogen-bonding interactions between the Br^- anion and the methine hydrogen are observed in the structures of **5** and **6**. In the case of **5**, the C(1)–H(1)···Br distances (corresponding angles) are 2.60 (147°), 2.49 (160°), and 2.39 Å (175°) for each of the three cations in the unit cell, while for **6** this distance is 2.52 Å (158°). These distances are all substantially less than the sum of the van der Waals radii, 2.99 Å [9].

Complexes **5** and **6** represent the first example of a matched isomer pair of poly(pyrazolyl)methane ligands which have been structurally characterized. In contrast, metal complexes that contain an asymmetrical arrangement of the ligand substituents are well-known in poly(pyrazolyl)borate chemistry [10]. Of all the poly(pyrazolyl)borate examples known, there appears to be only one case in which both isomers are

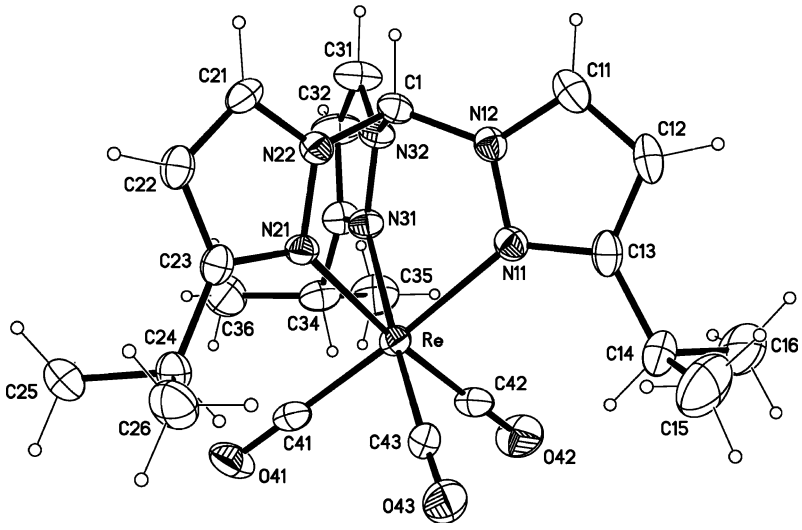

Fig. 2. ORTEP diagram of $\{[HC(3\text{-}i\text{-}Prpz)_3]Re(CO)_3\}^+$, cation A. Displacement ellipsoids drawn at the 50% probability level.

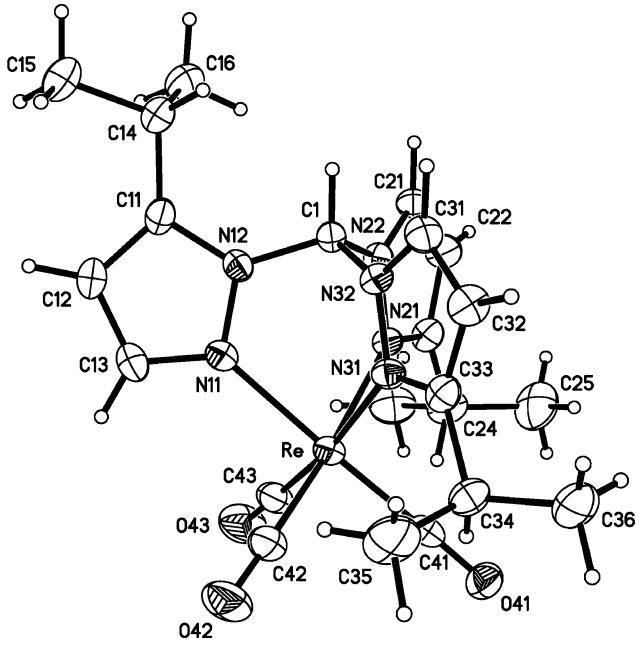

Fig. 3. ORTEP diagram of $\{[HC(3\text{-}i\text{-}Prpz)_2(5\text{-}i\text{-}Prpz)]Re(CO)_3\}^+$. Displacement ellipsoids drawn at the 50% probability level.

structurally characterized, $[HB(3\text{-}Cum\text{-}5\text{-}Mepz)_3]ZnSH$ and $[HB(3\text{-}Cum\text{-}5\text{-}Mepz)_2(3\text{-}Me\text{-}5\text{-}Cumpz)]ZnSH$ (Cum = *p*-isopropylphenyl) [10a]. These two tetrahedral complexes, despite the steric difference around their metal centers, have nearly identical structures.

Fig. 4 shows an ORTEP diagram of **10**, and selected bond distances and angles are collected in Table 3. The unit cell for **10** contains three crystallographically inequivalent but structurally similar $\{1,4\text{-}C_6H_4[CH_2OCH_2C(pz)_3]_2[Re(CO)_3]_2\}^{2+}$ cationic units. In this complex, which contains a bitopic ligand, the three nitrogen atoms from the pyrazolyl rings and three carbon atoms from the carbonyl ligands surround both rhenium atoms in a nearly octahedral arrangement. The average Re–N distance for **10** is 2.15 Å, the average N–Re–N angle is 81°, and the average OC–Re–CO angle is 89°. The overall arrangement of each bimetallic unit is a stepped structure formed by a *trans* arrangement of the two ether side arms about the linking arene group.

Table 2
Selected bond lengths (Å) and angles (°) for $\{[HC(3\text{-}i\text{-}Prpz)_3]Re(CO)_3\}Br\cdot(CH_3)_2CO$ (**5**), and $\{[HC(3\text{-}i\text{-}Prpz)_2(5\text{-}i\text{-}Prpz)]Re(CO)_3\}Br\cdot(CH_3)_2CO$ (**6**)

	5			**6**
	A	**B**	**C**	
Bond lengths				
Re–N(11)	2.187(3)	2.182(3)	2.180(3)	2.153(3)
Re–N(21)	2.195(3)	2.178(3)	2.192(3)	2.194(3)
Re–N(31)	2.182(3)	2.184(3)	2.183(3)	2.194(3)
Re–C(41)	1.896(5)	1.910(5)	1.909(4)	1.916(4)
Re–C(42)	1.925(5)	1.903(4)	1.900(5)	1.914(4)
Re–C(43)	1.917(5)	1.919(4)	1.916(5)	1.918(4)
Bond angles				
N(11)–Re–N(21)	82.42(12)	82.12(12)	81.77(12)	82.89(9)
N(11)–Re–N(31)	82.15(12)	83.73(12)	81.99(12)	81.24(10)
N(21)–Re–N(31)	80.66(12)	80.45(11)	83.48(12)	81.06(10)
C(41)–Re–C(42)	87.1(2)	88.56(18)	90.48(17)	89.03(14)
C(41)–Re–C(43)	87.5(2)	90.16(17)	89.88(18)	89.82(14)
C(42)–Re–C(43)	88.80(18)	90.89(17)	88.78(18)	87.95(15)
N(11)–Re–C(42)	95.43(16)	94.52(15)	94.35(15)	92.01(13)
N(11)–Re–C(43)	93.16(17)	91.36(15)	94.73(15)	92.26(13)
N(21)–Re–C(41)	94.97(17)	94.68(15)	93.14(15)	96.00(12)
N(21)–Re–C(43)	94.90(15)	94.08(14)	94.66(15)	94.22(12)
N(31)–Re–C(41)	97.02(18)	94.48(15)	93.27(15)	96.62(12)
N(31)–Re–C(42)	95.49(15)	94.35(15)	92.89(16)	96.23(13)
N(11)–Re–C(41)	177.35(16)	176.54(15)	173.38(15)	177.71(12)
N(21)–Re–C(42)	175.80(15)	174.05(15)	175.00(16)	174.52(12)
N(31)–Re–C(43)	173.90(17)	173.08(15)	176.42(16)	172.36(12)

Three nonequivalent cations (A, B, and C) are present in the crystal of **5**.

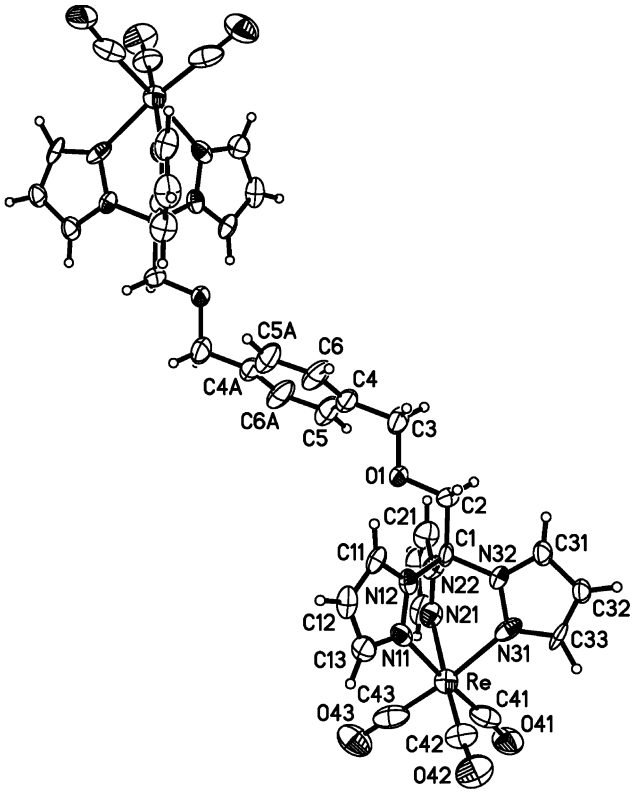

Fig. 4. ORTEP diagram of $\{1,4\text{-}C_6H_4[CH_2OCH_2C(pz)_3]_2[Re(CO)_3]_2\}^{2+}$, cation A. displacement ellipsoids drawn at the 30% probability level.

Table 3
Selected bond lengths (Å) and angles (°) for the three nonequivalent cations (A, B, and C) of $\{1,4\text{-}C_6H_4\ [CH_2OCH_2C(pz)_3]_2[Re(CO)_3]_2\}^{2+}$ (**10**)

	10		
	A	**B**	**C**
Bond lengths			
Re–N(11)	2.135(11)	2.135(13)	2.137(17)
Re–N(21)	2.150(11)	2.158(12)	2.140(13)
Re–N(31)	2.184(12)	2.151(11)	2.159(12)
Re–C(41)	1.900(17)	1.918(16)	1.89(2)
Re–C(42)	1.859(15)	1.81(2)	1.896(17)
Re–C(43)	1.80(2)	1.894(18)	1.93(2)
Bond angles			
N(11)–Re–N(21)	80.4(4)	81.5(4)	79.7(6)
N(11)–Re–N(31)	80.6(4)	81.1(4)	81.8(6)
N(21)–Re–N(31)	80.0(4)	81.8(4)	81.1(5)
C(41)–Re–C(42)	89.8(6)	91.8(7)	89.7(8)
C(41)–Re–C(43)	87.7(6)	89.1(7)	88.6(9)
C(42)–Re–C(43)	89.8(7)	88.2(9)	88.3(8)
N(11)–Re–C(42)	94.1(5)	95.3(6)	96.5(7)
N(11)–Re–C(43)	94.1(5)	93.8(6)	90.8(8)
N(21)–Re–C(41)	95.5(5)	91.2(6)	94.3(7)
N(21)–Re–C(43)	95.3(6)	97.8(7)	98.2(7)
N(31)–Re–C(41)	97.3(5)	96.1(5)	98.8(7)
N(31)–Re–C(42)	94.5(6)	91.9(7)	91.9(6)
N(11)–Re–C(41)	175.7(5)	172.5(6)	173.8(8)
N(21)–Re–C(42)	172.8(6)	173.4(6)	172.4(6)
N(31)–Re–C(43)	173.4(6)	174.8(6)	172.6(7)

Three cationic units, **A**, **B**, and **C**, are present in a 2:1:1 ratio and are organized into two similar 'zigzag' shaped chains by non-covalent interactions. The first type of chain is comprised of only the **A**-type cationic units (**A**–**A**), while the second chain is made up of alternating **B**- and **C**-type units (**B**–**C**). Each chain is formed by a series of π–π interactions between a pyrazolyl ring of one bimetallic building block and a pyrazolyl ring of an adjacent bimetallic building block. Fig. 5a and b show the **B**–**C** chain from two angles that are oriented 90° with respect to each other. The **A**–**A** chains are similar. Fig. 5a shows the interactions that hold the bimetallic units together in chains, while Fig. 5b displays the 'zigzag' shape of the chains due to the stepped structure of each individual unit. The pyrazolyl rings involved in the π–π interactions are parallel displaced with a centroid-to-centroid distance of 3.61 Å for the **A**–**A** chain and 3.70 Å for the **B**–**C** chain, with average centroid-to-ring plane perpendicular distances of 3.41 and 3.53 Å, respectively. These distances are well inside the 3.8 Å limit for π–π interactions [11].

The chains are also supported by (C)H···π interactions [12]. The pyrazolyl rings involved in the aforementioned π–π stacking have their 4-C(pz)–4-H(pz) bond directed toward another pyrazolyl ring of an adjacent unit. For the **A**–**A** chain, the (C)H···centroid distance is 2.85 Å (C–centroid distance of 3.70 Å) with a corresponding C–H··· centroid angle of 153°. For the **B**–**C** chain, there are two 4-C(pz)–4-H(pz) interactions, **B** to **C** and **C** to **B**. The (C)H(**B**)···centroid(**C**) distance is 2.78 Å (C–centroid distance of 3.62 Å) with a corresponding C–H(**B**)···centroid(**C**) angle of 150°, while the (C)H(**C**)···centroid(**B**) distance is 2.87 Å (C–centroid distance of 3.68 Å) with a corresponding C–H(**C**)···centroid(**B**) angle of 148°.

Fig. 6a and b show the orientation of the chains with respect to one another. Fig. 6a shows that the **A**–**A** and **B**–**C** chains are oriented in an interpenetrating 'zigzag' structure, with the two chains ca. one half of a bimetallic unit out of phase. Both chains run down the *a*-axis, Fig. 6b, with the 'planes' of each 'zigzag' chain oriented at a 69° angle with respect to one another. These two chains are held together by two types of pyrazolyl–arene–pyrazolyl π–π interactions, where the pyrazolyl rings sandwich the central arene ring. The pyrazolyl rings are parallel displaced (in opposite directions) above and below the plane of the arene (ar) ring. One interaction is between **C**(pz)–**A**(ar)–**C**(pz), while the other is between **A**(pz)–**B**(ar)–**A**(pz), Fig. 7. For the **A**–**B**–**A** interaction, the centroid-to-centroid distance is 3.77 Å with several C(pz)–C(ar) distances in the range of 3.40–3.80 Å, and an **A**(pz) plane–**B**(ar) plane angle of 19°. The **C**–**A**–**C** centroid-to-centroid distance is 3.77 Å with several C(pz)–C(ar) distances in the range of 3.48–3.80 Å, and a **C**(pz) plane–**A**(ar) plane angle of 21°. These π–π

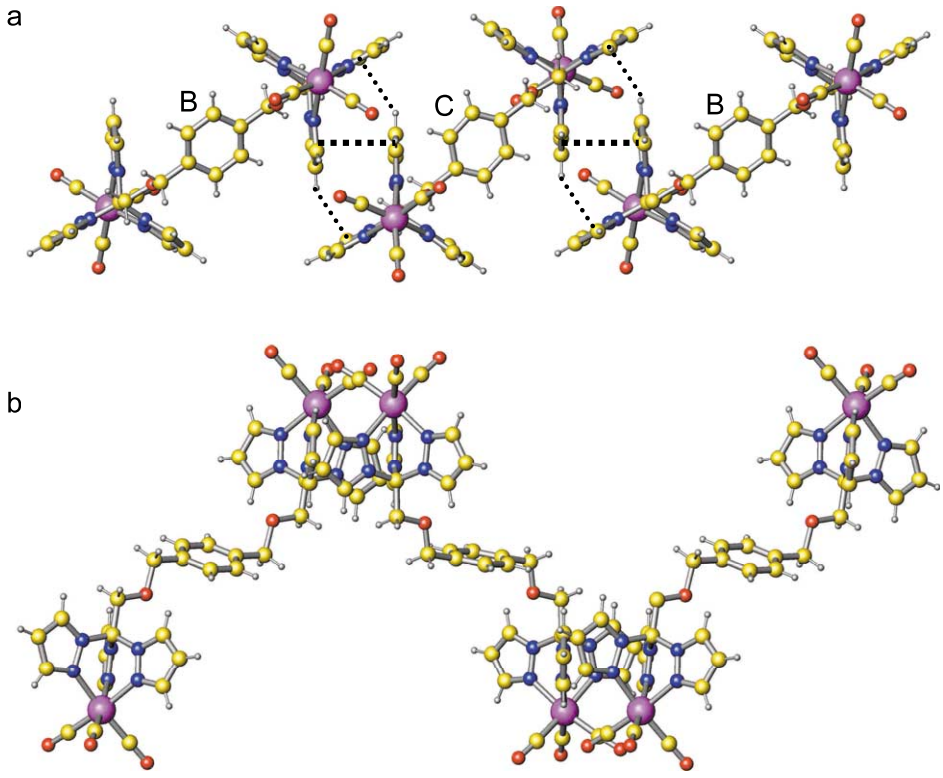

Fig. 5. (a) View of the **B**–**C** chain showing the π–π (dashed line) and (C)H···π (dotted line) interactions. (b) View of **B**–**C**, orthogonal to (a), showing the stepped structure of each unit, and the resulting 'zigzag' shape.

and (C)H···π interactions organize the bimetallic {1,4-C_6H_4 $[CH_2OCH_2C(pz)_3]_2[Re(CO)_3]_2\}^{2+}$ building blocks into a two-dimensional network. The Br^- counter-ions presumably further organize the organometallic building blocks into a 3D array, but since the anions were found to be disordered, detailed information on individual interactions is not available.

3. Experimental

All operations were carried out under a nitrogen atmosphere using either standard Schlenk techniques or a Vacuum Atmospheres HE-493 dry box. All solvents were dried and distilled prior to use. ^{1}H (400 MHz) and ^{13}C (101.62 MHz) NMR chemical shifts are reported in ppm versus TMS and referenced to the residual solvent peaks for $(CD_3)_2CO$, δ 2.06 (^{1}H) and δ 29.8 (^{13}C). The ^{13}C-NMR spectrum of **2** was acquired at −75 °C, whereas those of the remainder of the complexes were taken at room temperature (r.t.). Variable temperature ^{1}H- (500 MHz) NMR spectra of **10** were obtained in $DCON(CD_3)_2$ (DMF-d_7) with 10 μl TMS added as an internal standard. $Re(CO)_5Br$ was prepared by the literature procedure [13]. $HC(pz)_3$, $HC(3,5\text{-}Me_2pz)_3$, $HC(3\text{-}Phpz)_3$, $HC(3\text{-}i\text{-}Prpz)_3$–$HC(3\text{-}i\text{-}Prpz)_2(5\text{-}i\text{-}Prpz)$, $PhC(pz)_2(py)$, and 1,4-$C_6H_4[CH_2OCH_2C(pz)_3]_2$ were prepared according to our recently reported procedures [3c,6].

3.1. Synthesis of {[HC(pz)$_3$]Re(CO)$_3$}Br (1)

In a 100 ml Schlenk flask, $Re(CO)_5Br$ (0.30 g, 0.74 mmol) and $HC(pz)_3$ (0.16 g, 0.74 mmol) were dissolved in toluene (15 ml). The resulting solution was stirred and heated at reflux for 20 h. During this time, a white solid precipitated. The slurry was allowed to cool to r.t. and filtered. The remaining solid was washed with toluene (3 × 5 ml) and dried in vacuo to yield a white solid (0.38 g, 91%). Melting point (m.p.) 310 °C (dec.). The preparation of this compound in ethanol has been briefly mentioned, although no spectral characterization was presented [5]. ^{1}H-NMR(acetone-d_6): δ 13.04 (s, 1H, *H*C), 9.04, 8.53 (d, d, 3H, 3H, $J = 2.4$, 2.4 Hz, 3,5-*H* pz), 6.75 (dd, 3H, $J = 2.4$ Hz, 4-*H* pz). ^{13}C-NMR (acetone-d_6): δ 148.1 (3-C pz), 134.7 (5-C pz), 109.1 (4-C pz), 73.9 (H*C*). IR(CH_2Cl_2, ν(CO), cm^{-1}): 2042 (s), 1938 (m). Accurate FAB$^+$MS Calc. for [M^+], [$C_{13}H_{10}N_6O_3{}^{187}Re]^+$, 485.0372. Found: 485.0392.

3.2. Synthesis of {[HC(pz)$_3$]Re(CO)$_3$}BF$_4$ (2)

In a 100 ml Schlenk flask wrapped in aluminum foil, $Re(CO)_5Br$ (0.20 g, 0.49 mmol) and $AgBF_4$ (0.095 g, 0.49 mmol) were dissolved in DME (40 ml). The

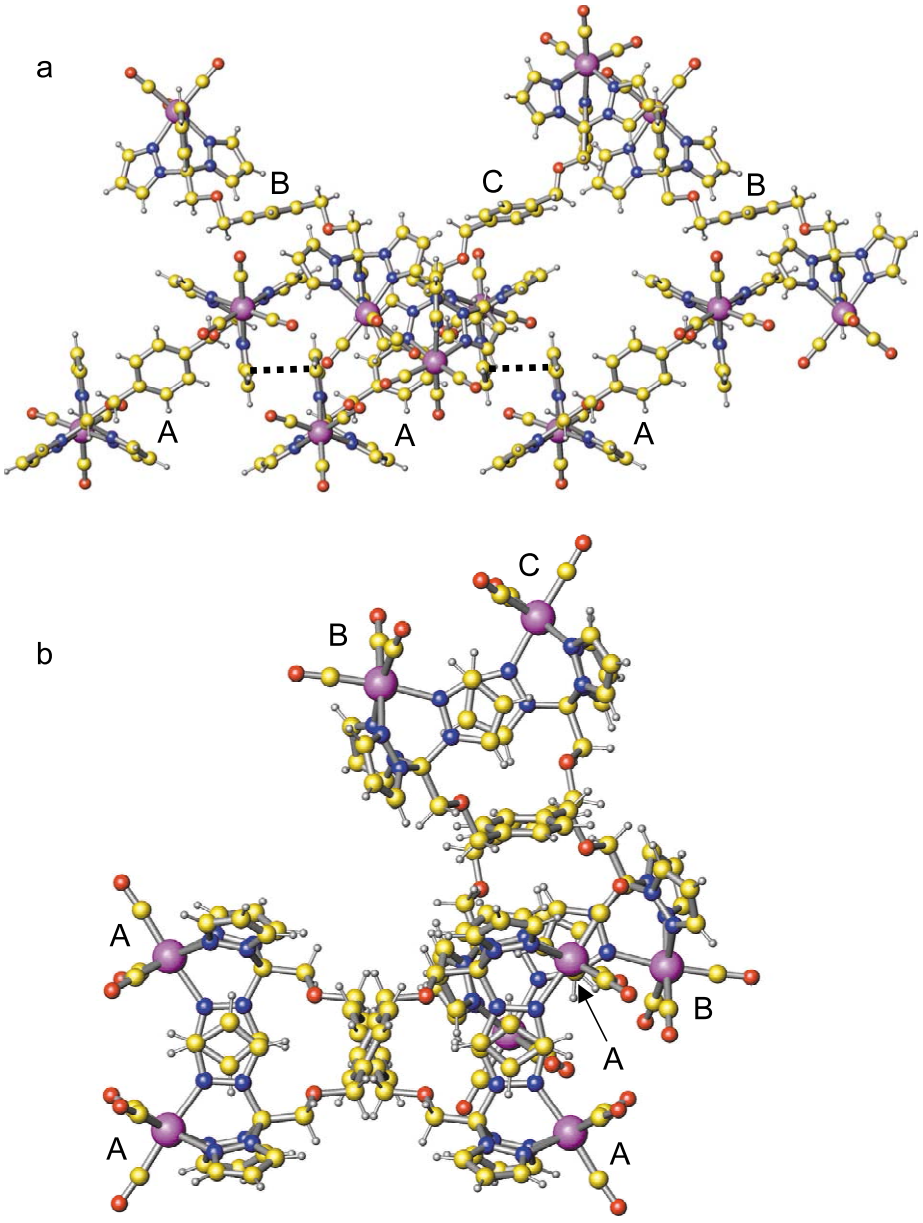

Fig. 6. Views of **A**–**A** and **B**–**C** chains with respect to each other. (a) The **A**–**A** chain is in the same orientation as Fig. 5a, with the corresponding π–π (dashed line) interactions shown. The **B**–**C** chain is in a similar orientation to Fig. 5b. (b) View down the chains (*a*-axis) of the **A**–**A** and **B**–**C** chains, orthogonal to (a). In the picture, the **A**–**A** chain is horizontal, and the **B**–**C** chain is nearly vertical.

solution was stirred and heated at reflux for 40 h. AgBr was removed by cannula filtration, and the clear, colorless filtrate was added to a flask that contained $HC(pz)_3$ (0.10 g, 0.49 mmol). The resulting solution was stirred and heated at reflux for 4 h during which time a precipitate appeared. The solvent was removed in vacuo yielding an off-white solid. The solid was dissolved in CH_2Cl_2 (30 ml), and hexane (60 ml) was added to precipitate the desired product. The solid was collected and dried under vacuum yielding a white solid (0.19 g, 66%). M.p. 250 °C (dec.). ^{1}H-NMR (acetone-d_6): δ 9.88 (s, 1H, *H*C), 8.64, 8.61 (d, d, 3H, 3H, $J = 2.4$ Hz, $J = 2.4$ Hz, 3,5-*H* pz), 6.78 (dd, 3H, $J = 2.4$ Hz, 4-*H* pz). ^{13}C-NMR (acetone-d_6): δ 197.3 (CO), 148.7 (3-C pz), 135.6 (5-C pz), 109.4 (4-C pz), 77.1 (H*C*). IR(CH_2Cl_2, ν(CO), cm^{-1}): 2043 (s), 1938 (m). Accurate ES$^+$MS Calc. for $[M^+]$, $[C_{13}H_{10}N_6O_3{}^{185}Re]^+$, 483.0344. Found: 483.0352.

3.3. Synthesis of {[HC(3,5-Me$_2$pz)$_3$]Re(CO)$_3$}Br (**3**)

This compound was prepared (0.36 g, 74%) as described above for **1** using $Re(CO)_5Br$ (0.30 g, 0.74 mmol) and $HC(3,5\text{-}Me_2pz)_3$ (0.22 g, 0.74 mmol). M.p. 250 °C (dec.). ^{1}H-NMR(acetone-d_6): δ 8.31 (s, 1H, *H*C), 6.47 (s, 3H, 4-*H* pz), 2.86, 2.56 (s, s, 9H, 9H, 3,5-

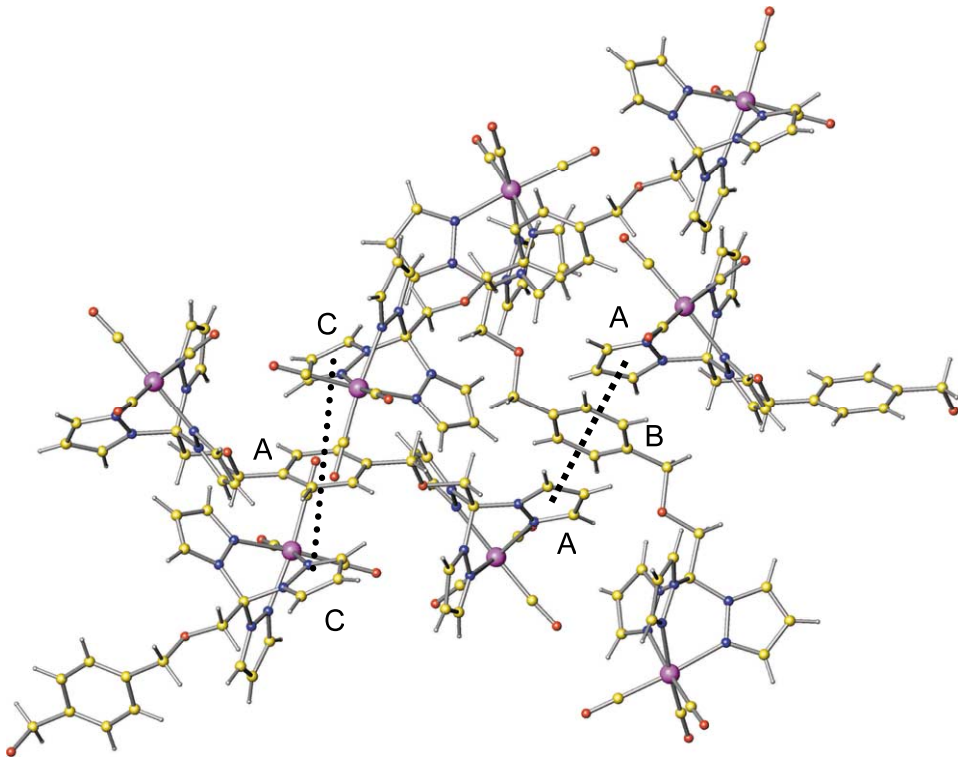

Fig. 7. View showing the C(pz)–A(ar)–C(pz) π–π (dotted line) interaction and the A(pz)–B(ar)–A(pz) π–π (dashed line).

Me). IR(CH_2Cl_2, ν(CO), cm^{-1}): 2036 (s), 1930 (m). Accurate FAB$^+$MS Calc. for [M^+], [$C_{19}H_{22}N_6O_3{}^{185}Re$]$^+$, 567.1283. Found: 567.1298.

3.4. Synthesis of {[HC(3-Phpz)$_3$]Re(CO)$_3$}Br (**4**)

This compound was prepared (0.43 g, 73%) as described above for **1** using $Re(CO)_5Br$ (0.30 g, 0.74 mmol) and HC(3-Phpz)$_3$ (0.33 g, 0.74 mmol). M.p. 240 °C (dec.). ^{1}H-NMR (acetone-d_6): δ 10.68 (s, 1H, *H*C), 9.49 (d, 3H, $J = 2.4$ Hz, 5-*H* (pz)), 7.47–7.57 (m, 15H, C_6H_5), 6.75 (d, 3, $J = 2.4$ Hz, 4-*H* (pz)). IR(CH_2Cl_2, ν(CO), cm^{-1}): 2040 (s), 1934 (m). Accurate FAB$^+$MS Calc. for [M^+], [$C_{31}H_{22}N_6O_3{}^{187}Re$]$^+$, 713.1312. Found: 713.1302.

3.5. Synthesis of {[HC(3-i-Prpz)$_3$]Re(CO)$_3$}Br (**5**) and {[HC(3-i-Prpz)$_2$(5-i-Prpz)]Re(CO)$_3$}Br (**6**)

In a 100 ml Schlenk flask, $Re(CO)_5Br$ (0.30 g, 0.74 mmol) and a 4:1 mixture of HC(3-*i*-Prpz)$_3$–HC(3-*i*-Prpz)$_2$(5-*i*-Prpz) (0.31 g, 0.90 mmol) were dissolved in toluene (40 ml). The orange solution was stirred and heated at reflux for 20 h, was cooled to r.t., and solvent was removed in vacuo. The remaining brown solid was washed with diethyl ether (3×10 ml) to remove unreacted starting materials, and the resulting white solid (0.32 g, 63%) was dried in vacuo. NMR analysis showed the solid to be 85% **5** and 15% **6**. Crystals suitable for X-ray analysis were grown by slow evaporation of an acetone solution, and the crystals used for the structural determinations of **5** and **6** were mechanically separated from the same vial. ^{1}H-NMR (acetone-d_6) for **5**: δ 12.69 (s, 1H, *H*C), 8.93 (d, 3H, $J = 2.8$ Hz, 5-*H* pz), 6.72 (d, 3H, $J = 2.8$ Hz, 4-*H* pz), 3.50 (septet, 3H, $J =$ 6.8 Hz, C*H*(CH$_3$)$_2$), 1.35 (d, 18H, $J = 6.8$ Hz, CH(C*H*$_3$)$_2$). ^{13}C-NMR (acetone-d_6) for **5**: δ 166.9 (3-*C* pz), 135.0 (5-*C* pz), 105.1 (4-*C* pz), 73.6 (H*C*), 30.1 (*C*H(CH$_3$)$_2$), 22.5 (CH(*C*H$_3$)$_2$). ^{1}H-NMR(acetone-d_6) for **6**: δ 12.09 (s, 1H, *H*C), 9.48 (d, 2H, $J = 3.2$ Hz, 5-*H* 3-*i*-Prpz), 8.40 (d, 1H, $J = 2.4$ Hz, 3-*H* 5-*i*-Prpz), 6.70 (d, 2H, $J = 3.2$ Hz, 4-*H* 3-*i*-Prpz), 6.57 (d, 1H, $J = 2.4$ Hz, 4-*H* 5-*i*-Prpz), 4.39 (septet, 1H, $J = 6.8$ Hz, C*H*(CH$_3$)$_2$ 5-*i*-Prpz), 3.40 (septet, 2H, $J = 6.8$ Hz, C*H*(CH$_3$)$_2$ 3-*i*-Prpz), 1.36 (d, 12H, $J = 6.8$ Hz, CH(C*H*$_3$)$_2$ 3-*i*-Prpz), 1.33 (d, 6H, $J = 6.8$ Hz, CH(C*H*$_3$)$_2$ 5-*i*-Prpz). IR(CH_2Cl_2, ν(CO), cm^{-1}): 2037 (s), 1930 (m). Accurate FAB$^+$MS Calc. for [M^+], [$C_{22}H_{28}N_6O_3{}^{187}Re$]$^+$, 611.1781. Found: 611.1786.

3.6. Synthesis of {[HC(3-i-Prpz)$_3$]Re(CO)$_3$}BF$_4$ (**7**) and {[HC(3-i-Prpz)$_2$(5-i-Prpz)]Re(CO)$_3$}BF$_4$ (**8**)

In a 100 ml Schlenk flask wrapped in aluminum foil, $Re(CO)_5Br$ (0.41 g, 1.0 mmol) and $AgBF_4$ (0.20 g, 1.0 mmol) were dissolved in DME (40 ml). The solution was stirred and heated at reflux for 36 h. AgBr was removed by cannula filtration, and the colorless filtrate was

added to a flask that contained a 4:1 HC(3-*i*-Prpz)$_3$–HC(3-*i*-Prpz)$_2$(5-*i*-Prpz) mixture (0.34 g, 1.0 mmol). The yellow–orange solution was stirred and heated at reflux for 8 h, cooled to r.t., and solvent was removed in vacuo yielding a light brown oil. NMR analysis of the crude mixture showed the solid to be 80% **7** and 20% **8**. The solid was dissolved in CH_2Cl_2 (10 ml), and hexane (50 ml) was added. After filtration, the remaining off-white solid (0.23 g, 32%) was dried under vacuum and was shown by NMR to be pure **7**. M.p. 200 °C (dec.). ^{1}H-NMR (acetone-d_6) for **7**: δ 9.47 (s, 1H, *H*C), 8.48 (d, 3H, $J = 2.8$ Hz, 5-*H* pz), 6.75 (d, 3H, $J = 2.8$ Hz, 4-*H* pz), 3.52 (septet, 3H, $J = 6.8$ Hz, C*H*(CH$_3$)$_2$), 1.36 (d, 18H, $J = 6.8$, CH(C*H*$_3$)$_2$). ^{13}C-NMR (acetone-d_6) for **7**: δ 167.5 (3-*C* pz), 135.9 (5-*C* pz), 105.7 (4-*C* pz), 77.2 (H*C*), 30.2 (*C*H(CH$_3$)$_2$), 22.5 (CH(*C*H$_3$)$_2$). ^{1}H-NMR (acetone-d_6) for **8**: δ 9.46 (s, 1H, *H*C), 8.58 (d, 2H, $J =$ 3.2 Hz, 5-*H* 3-*i*-Prpz), 8.48 (d, 1H, $J = 2.4$ Hz, 3-*H* 5-*i*-Prpz), 6.77 (d, 2H, $J = 3.2$ Hz, 4-*H* 3-*i*-Prpz), 6.64 (d, 1H, $J = 2.4$ Hz, 4-*H* 5-*i*-Prpz), 3.76 (septet, 1H, $J = 6.8$ Hz, C*H*(CH$_3$)$_2$ 5-*i*-Prpz), 3.12 (septet, 2H, $J = 6.8$ Hz, C*H*(CH$_3$)$_2$ 3-*i*-Prpz), 1.36 (d, 12H, $J = 6.8$ Hz, CH(C*H*$_3$)$_2$ 3-*i*-Prpz), 1.34 (d, 6H, $J = 6.8$ Hz, CH(C*H*$_3$)$_2$ 5-*i*-Prpz). IR (CH_2Cl_2, ν(CO), cm^{-1}): 2037 (s), 1932 (m). Accurate ES$^+$MS Calc. for [M$^+$], [$C_{22}H_{28}N_6O_3{}^{185}$Re]$^+$, 609.1753. Found: 609.1750.

3.7. Synthesis of {[PhC(pz)$_2$(py)]Re(CO)$_3$}Br (9)

This compound was prepared (0.20 g, 61%) as described above for the **5**–**6** mixture using Re(CO)$_5$Br (0.20 g, 0.50 mmol) and PhC(pz)$_2$(py) (0.15 g, 0.50 mmol. M.p. 230 °C (dec.). ^{1}H-NMR (acetone-d_6, individual resonances could not be assigned due to the complexity of the spectrum): complex resonances centered at δ 9.37, 8.58, 8.24, 8.21, 7.94, 7.75, 7.65, 7.49, 6.65, 6.20. IR(CH_2Cl_2, ν(CO), cm^{-1}): 2026 (s), 1922 (m), 1899 (m). Accurate FAB$^+$MS Calc. for [M$^+$], [$C_{21}H_{15}N_5O_3{}^{187}$Re]$^+$, 572.0733. Found: 572.0731.

3.8. Synthesis of {1,4-C$_6$H$_4$[CH$_2$OCH$_2$C(pz)$_3$]$_2$[Re(CO)$_3$]$_2$}Br$_2$ (10)

This compound was prepared (0.30 g, 77%) as described above for the **5**–**6** mixture using Re(CO)$_5$Br (0.24 g, 0.60 mmol) and 1,4-C$_6$H$_4$[CH$_2$OCH$_2$C(pz)$_3$]$_2$ (0.18 g, 0.30 mmol). M.p. 225 °C (dec.). ^{1}H-NMR (acetone-d_6, ambient): δ 9.10, 8.89 (2H, 4H, 5-*H* pz), 8.52 (6H, 3-*H* pz), 7.64 (s, 4H, C$_6$*H*$_4$), 6.70, 6.66 (2H, 4H, 4-*H* pz), 6.36 (s, 4H, OC*H*$_2$Ph), 5.47 (s, 4H, OC*H*$_2$C(pz)$_3$ ^{1}H-NMR (DMF-d_7, -5 °C): δ 9.10, 9.07 (d, d, 2H, 4H, $J = 3.0$, 3.0 Hz, 5-*H* pz), 8.90, 8.88 (d, d, 2H, 4H, $J = 2.5$, 2.0 Hz, 3-*H* pz), 7.65 (s, 4H, C$_6$*H*$_4$), 6.94, 6.90 (dd, dd, 2H, 4H, $J = 2.5$, 3.0 Hz; $J = 2.5$, 3.0 Hz, 4-*H* pz), 6.16 (s, 4H, OC*H*$_2$Ph), 5.31 (s, 4H, OC*H*$_2$C(pz)$_3$). IR (CH_2Cl_2, ν(CO)): 2042 cm^{-1} (s), 1938 cm^{-1} (m). Accurate FAB$^+$MS Calc. for [M], [$C_{36}H_{30}BrN_{12}O_8{}^{185}Re_2$]$^+$, 1207.0552. Found: 1207.0557.

4. Crystallographic studies

Single crystals of **5**, **6**, and **10** were grown by slow evaporation of a saturated acetone solution of each complex. Crystal, data collection, and refinement parameters are given in Table 4. An irregular colorless crystal of **5** and a colorless plate crystal of **6** were mounted on the ends of thin glass fibers using inert oil, and quickly transferred to the diffractometer cold stream for data collection at 173(2) K. For **10**, a colorless bar was epoxied to the end of a glass fiber for data collection at 293 K. Raw X-ray intensity data frames were measured on a Bruker SMART APEX CCD-based diffractometer system (Mo–K$_\alpha$ radiation, $\lambda = 0.71073$ Å). The raw data frames were integrated using SAINT+ [14], which also applied corrections for Lorentz and polarization effects. Analysis of the data sets showed negligible crystal decay during data collection in any case. An empirical absorption correction based on the multiple measurement of equivalent reflections was applied to each data set with the program SADABS [15]. All structures were solved by a combination of direct methods and difference Fourier syntheses, and refined by full-matrix least-squares against F^2, using the SHELXTL software package [15].

{[HC(3-*i*-Prpz)$_3$]Re(CO)$_3$}Br·(CH$_3$)$_2$CO (**5**), crystallizes in the triclinic system; the space group $P\bar{1}$ was assumed and confirmed by successful solution and refinement of the structure. {[HC(3-*i*-Prpz)$_2$(5-*i*-Prpz)]Re(CO)$_3$}Br·(CH$_3$)$_2$CO (**6**), crystallizes in the space group $P2_1/c$ as determined by the systematic absences in the intensity data, with one {[HC(3-*i*-Prpz)$_2$(5-*i*-Prpz)]Re(CO)$_3$}Br moiety and one acetone molecule of crystallization in the asymmetric unit. The asymmetric unit of **5** contains three crystallographically independent {[HC(3-*i*-Prpz)$_3$]Re(CO)$_3$}Br moieties and three acetone molecules of crystallization. Six restraints were employed via a SHELX SAME instruction to maintain a chemically reasonable geometry for one of the acetones. Eventually, all non-hydrogen atoms were refined with anisotropic displacement parameters; hydrogen atoms were placed in idealized positions and refined using a riding model.

{1,4-C$_6$H$_4$[CH$_2$OCH$_2$C(pz)$_3$]$_2$[Re(CO)$_3$]$_2$}(Br)$_2$ (**10**), crystallizes in the monoclinic space group *I*2/*a* based on systematic absences. The space group *I*2/*a* is a non-standard setting of *C*2/*c* and was chosen to give a more orthogonal cell. Three crystallographically inequivalent but chemically similar {1,4-C$_6$H$_4$-[CH$_2$OCH$_2$-C(pz)$_3$]$_2$[Re(CO)$_3$]$_2$}$^{2+}$ cations were located. All three are situated about centers of symmetry, and, therefore,

Table 4
Crystal data and structure refinement for {[HC(3-*i*-Prpz)$_3$]Re(CO)$_3$}Br·(CH$_3$)$_2$CO (**5**), {[HC(3-*i*-Prpz)$_2$(5-*i*-Prpz)]Re(CO)$_3$}Br·(CH$_3$)$_2$CO (**6**), and {1,4-C$_6$H$_4$ [CH$_2$OCH$_2$C(pz)$_3$]$_2$[Re(CO)$_3$]$_2$}Br$_2$ (**10**)

	5	**6**	**10**
Empirical formula	$C_{25}H_{34}BrN_6O_4Re$	$C_{25}H_{34}BrN_6O_4Re$	$C_{36}H_{30}Br_2N_{12}O_8Re_2$
Formula weight	748.69	748.69	1290.94
Temperature (K)	173(2)	173(2)	293(2)
Wavelength (Å)	0.71073	0.71073	0.71073
Crystal system	triclinic	monoclinic	monoclinic
Space group	$P\bar{1}$	$P2_1/c$	$I2/a$
Unit cell dimensions			
a(Å)	12.8953(8)	15.9401(11)	23.0216(17)
b(Å)	19.2725(12)	12.3926(9)	21.2920(16)
c(Å)	19.4746(12)	16.0470(11)	30.813(3)
α(°)	76.0720(10)	90	90
β(°)	72.0680(10)	113.8110(10)	93.1930(10)
γ(°)	85.8090(10)	90	90
V (Å^3)	4469.4(5)	2900.1(4)	15080(2)
Z	6	4	12
Density (calculated) (g cm^{-3})	1.669	1.715	1.706
Absorption coefficient (mm^{-1})	5.458	5.608	6.456
Crystal size (mm^3)	0.40 × 0.22 × 0.12	0.20 × 0.13 × 0.05	0.22 × 0.08 × 0.05
θ range for data collection (°)	1.38–26.39	2.15–26.40	1.82–25.11
Index ranges	$-16 \le h \le 16$, $-24 \le k \le 24$, $-24 \le l \le 24$	$-17 \le h \le 19$, $-15 \le k \le 13$, $-20 \le l \le 17$	$-22 \le h \le 27$, $-25 \le k \le 23$, $-36 \le l \le 36$
Reflections collected	41 399	19 019	44 981
Independent reflections	18 233 [$R_{int} = 0.0334$]	5932 [$R_{int} = 0.0332$]	13 382 [$R_{int} = 0.0731$]
Completeness to $\theta = 26.4°$	99.6%	99.8%	99.4%
Absorption correction	Semi-empirical from equivalents	Semi-empirical from equivalents	Semi-empirical from equivalents
Max/min transmission	0.6220 and 0.4029	0.8250 and 0.5424	0.7384 and 0.3309
Data/restraints/parameters	18 233/6/1024	5932/0/341	13 382/0/847
Goodness-of-fit on F^2	1.011	1.003	1.007
Final R indices [$I > 2\sigma(I)$]	$R_1 = 0.0302$, $wR_2 = 0.0509$	$R_1 = 0.0249$, $wR_2 = 0.0484$	$R_1 = 0.0560$, $wR_2 = 0.1176$
R indices (all data)	$R_1 = 0.0396$, $wR_2 = 0.0519$	$R_1 = 0.0314$, $wR_2 = 0.0495$	$R_1 = 0.1186$, $wR_2 = 0.1232$
Largest difference peak and hole (e Å^{-3})	1.401 and −1.105	0.977 and −0.569	0.940 and −1.274

only half of each is present in the asymmetric unit. The inversion centers reside at the centroid of the phenyl ring in each ligand. The packing of the {1,4-C$_6$H$_4$[CH$_2$OCH$_2$C(pz)$_3$]$_2$[Re(CO)$_3$]$_2$}$^{2+}$ cations generates sizable channels running along the crystallographic a axis, which contain the bromine counterions and the solvent molecules. Significant positional disorder was observed for two of the three bromine counterions per asymmetric unit (Br2$^-$ and Br3$^-$). Both were found to be disordered over three partially occupied sites. Their site occupation factors were adjusted to give reasonable thermal parameters, with the constraint of summing to unity. Further severe disorder afflicts the acetone solvent molecules, for which no reasonable solution could be obtained despite several attempted models. These were accounted for using the SQUEEZE [16] program in PLATON [17] for modeling diffusely scattering solvent molecules. The program calculated a solvent-accessible volume in the unit cell of 3138.8 Å^3 (20.8% of the total cell volume), corresponding to 962 electrons, which in turn corresponds to 30 acetone molecules per cell. The contribution of these diffuse solvent molecules was then subtracted from the structure factor calculations. Eventually, all non-hydrogen atoms were refined with anisotropic displacement parameters; all hydrogen atoms were placed in idealized positions and refined using a riding model. Note that the tabulated crystallographic data reflect only the known cell contents.

5. Supplementary material

Crystallographic data for the structural analysis has been deposited with the Cambridge crystallographic Centre, CCDC 181222 for compound **5**, CCDC 181223 for compound **6**, and CCDC 181224 for compound **10**. Copies of this information may be obtained free of charge from the director, CCDC, 12 Union Road, Cambridge, CB2 1EZ UK (Fax: +44-1223-336033; e-mail: deposit@ccdc.cam.ac.uk or www: http://www.ccdc.cam.ac.uk.

Acknowledgements

We thank the National Science Foundation (CHE-0110493) for support. The Bruker CCD Single Crystal Diffractometer was purchased using funds provided by the NSF Instrumentation for Materials Research Program through Grant DMR:9975623. The NSF (Grants CHE-8904942 and CHE-9601723) and NIH (Grant RR-02425) have supplied funds to support NMR equipment and the NIH (Grant RR-02849) has supplied funds to support mass spectrometry equipment at the University of South Carolina.

References

[1] (a) D.L. Reger, J.E. Collins, A.L. Rheingold, L.M. Liable-Sands, Organometallics 15 (1996) 2029;
(b) D.L. Jameson, R.K. Castellano, Inorg. Syn. 32 (1998) 51;
(c) C. Titze, J. Hermann, H. Vahrenkamp, Chem. Ber. 118 (1995) 1095;
(d) D.L. Reger, J.E. Collins, R. Layland, R.D. Adams, Inorg. Chem. 35 (1996) 1372;
(e) D.L. Reger, J.E. Collins, M.A. Matthews, A.L. Rheingold, L.M. Liable-Sands, L.A. Guzei, Inorg. Chem. 36 (1997) 6226;
(f) D.L. Reger, Comm. Inorg. Chem. 21 (1999) 1;
(g) D.L. Reger, C.A. Little, A.L. Rheingold, M. Lam, T. Concolino, A. Mohan, G.J. Long, Inorg. Chem. 39 (2000) 4674;
(h) D.L. Reger, C.A. Little, A.L. Rheingold, M. Lam, L.M. Liable-Sands, B. Rhagitan, T. Concolino, A. Mohan, G.J. Long, V. Briois, F. Grandjean, Inorg. Chem. 40 (2001) 1508;
(i) P.K. Byers, A.J. Canty, R.T. Honeyman, Adv. Organomet. Chem. 34 (1992) 1.

[2] (a) S. Trofimenko, Acc. Chem. Res. 4 (1971) 17;
(b) S. Trofimenko, J. Am. Chem. Soc. 89 (1967) 3170;
(c) S. Trofimenko, J. Am. Chem. Soc. 89 (1967) 6288;
(d) A.J. Shaver, Organomet. Chem. Lib. 3 (1976) 157;
(e) S. Trofimenko, Prog. Inorg. Chem. 34 (1988) 115;
(f) S. Trofimenko, Chem. Rev. 93 (1993) 943;
(g) S. Trofimenko, J.C. Calabrese, J.S. Thompson, Inorg. Chem. 26 (1987) 1507;
(h) S. Trofimenko, Scorpionates—The Coordination Chemistry of Poly(pyrazolyl)borate Ligands, Imperial College, London, 1999;
(i) A.S. Lipton, S.S. Mason, S.M. Myers, D.L. Reger, P.D. Ellis, Inorg. Chem. 35 (1996) 7111;
(j) D.L. Reger, S.M. Myers, S.S. Mason, D.J. Darensbourg, M.W. Holtcamp, J.H. Reibenspeis, A.S. Lipton, P.D. Ellis, J. Am. Chem. Soc. 117 (1995) 10998;
(k) D.L. Reger, S.M. Myers, S.S. Mason, A.L. Rheingold, B.S. Haggerty, P.D. Ellis, Inorg. Chem. 34 (1995) 4996;
(l) D.L. Reger, S.S. Mason, A.L. Rheingold, Inorg. Chim. Acta 240 (1995) 669;
(m) A.S. Lipton, S.S. Mason, D.L. Reger, P.D. Ellis, J. Am. Chem. Soc. 116 (1994) 10182.

[3] (a) D.L. Reger, J.E. Collins, D.L. Jameson, R.K. Castellano, Inorg. Syn. 32 (1998) 63;
(b) D.L. Reger, J.E. Collins, A.L. Rheingold, L.M. Liable-Sands, G.P.A. Yap, Organometallics 16 (1997) 349;
(c) D.L. Reger, T.C. Grattan, K.J. Brown, C.A. Little, J.J.S. Lamba, A.L. Rheingold, R.D. Sommer, J. Organomet. Chem. 607 (2000) 120;
(d) D.L. Reger, J.E. Collins, S.M. Myers, A.L. Rheingold, L.M. Liable-Sands, Inorg. Chem. 35 (1996) 4904.

[4] (a) V.W.W. Yam, Y. Yang, H.P. Yang, K.K. Cheung, Organometallics 18 (1999) 5252;
(b) S.S. Sun, A.S. Silva, I.M. Brinn, A.J. Lees, Inorg. Chem. 39 (2000) 1344;
(c) A. Rey, I. Pirmettis, M. Pelecanou, M. Papadopoulos, C.P. Raptopoulou, L. Mallo, C.I. Stassinopoulou, A. Terzis, E. Chiotellis, A. Leon, Inorg. Chem. 39 (2000) 4211;
(d) M. Kohlickova, V. Jedinakova-Krizova, F. Melichar, Chem. Listy 94 (2000) 151;
(e) K. Hashimoto, K. Yoshihara, Top. Curr. Chem. 176 (1996) 275.

[5] D.H. Gibson, M.S. Mashuta, H. He, Acta Crystallogr. Sect. C 57 (2001) 1135.

[6] (a) D.L. Reger, T.D. Wright, R.F. Semeniuc, T.C. Grattan, M.D. Smith, Inorg. Chem. 40 (2001) 6212;
(b) D.L. Reger, R.F. Semeniuc, M.D. Smith, Eur. J. Inorg. Chem. (2002) 543.

[7] S.B. Seymore, S.N. Brown, Inorg. Chem. 39 (2000) 325.

[8] (a) H. Kessler, Angew. Chem. Int. Ed. Eng. 9 (1970) 219;
(b) M.L. Martin, G.J. Martin, J.J. Delpuech, Practical NMR Spectroscopy, Heyden, London, 1980.

[9] (a) A. Bondi, J. Phys. Chem. 68 (1964) 441;
(b) R.S. Rowland, R. Taylor, J. Phys. Chem. 100 (1996) 7384.

[10] (a) M. Ruf, H. Vahrenkamp, Inorg. Chem. 35 (1996) 6571;
(b) J.C. Calabrese, S. Trofimenko, Inorg. Chem. 31 (1992) 4810;
(c) A.L. Rheingold, C.B. White, S. Trofimenko, Inorg. Chem. 32 (1993) 3471;
(d) D.D. LeCloux, M.C. Keyes, M. Osawa, V. Reynolds, W.B. Tolman, Inorg. Chem. 33 (1994) 6361;
(e) R. Han, G. Parkin, S. Trofimenko, Polyhedron 14 (1995) 387;
(f) C.G. Young, L.J. Laughlin, S. Colmanet, S.D.B. Scrofani, Inorg. Chem. 35 (1996) 5368;
(g) M.H. Chisholm, N.W. Eilerts, J.C. Huffman, Inorg. Chem. 35 (1996) 445;
(h) D.J. Darensbourg, E.L. Maynard, M.W. Holtcamp, K.K. Klausmeyer, J.H. Reibenspies, Inorg. Chem. 35 (1996) 2682;
(i) A.L. Rheingold, L.M. Liable-Sands, G.P.A. Yap, S. Trofimenko, Chem. Commun. (1996) 1233;
(j) A.L. Rheingold, B.S. Haggerty, G.P.A. Yap, S. Trofimenko, Inorg. Chem. 36 (1997) 5097.

[11] C. Janiak, J. Chem. Soc. Dalton Trans. (2000) 3885 and references therein.

[12] (a) H. Takahashi, S. Tsuboyama, Y. Umezawa, K. Honda, M. Nishio, Tetrahedron 56 (2000) 6185;
(b) S. Tsuzuki, K. Honda, T. Uchimaru, M. Mikami, K.J. Tanabe, Am. Chem. Soc. 122 (2000) 11450;
(c) O. Seneque, M. Giorgi, O. Reinaud, Chem. Commun. (2001) 984;
(d) H.C. Weiss, D. Blaser, R. Boese, B.M. Doughan, M.M. Haley, Chem. Commun. (1997) 1703;
(e) N.N.L. Madhavi, A.K. Katz, H.L. Carrell, A. Nangia, G.R. Desiraju, Chem. Commun. (1997) 2249;
(f) N.N.L. Madhavi, A.K. Katz, H.L. Carrell, A. Nangia, G.R. Desiraju, Chem. Commun. (1997) 1953.

[13] S.P. Schmidt, W.C. Trogler, F. Basolo, Inorg. Syn. 28 (1990) 160.

[14] SAINT+ Version 6.02a. Bruker Analytical X-ray Systems, Inc., Madison WI, USA, 1998.

[15] G.M. Sheldrick, SHELXTL Version 5.1, Bruker Analytical X-ray Systems, Inc, Madison WI, USA, 1997.

[16] SQUEEZE. P. Sluis v.d., A.L. Spek, Acta Crsytallogr. Sect. A 46 (1990) 194.

[17] PLATON. A.L. Spek, Acta Crystallogr. Sect. A 46(1990) C-34.